Biosorption of methyl violet from aqueous solution using Algerian biomass

A. Hamitouche, S. Benammar , M. Haffas, A. Boudjemaa*, K. Bachari

*Research Centre in Analytical Chemistry Physics (CRAPC), BP 248, Algiers RP 16004, Algeria, Tel. +213 21 24 74 06;
Fax: +213 24 46 36 93; emails: ahamitouche2@yahoo.fr (A. Hamitouche), souad.benammar@yahoo.fr (S. Benammar),
youba54@yahoo.com (M. Haffas), amel_boudjemaa@yahoo.fr (A. Boudjemaa), bachari2000@yahoo.fr (K. Bachari)*

ABSTRACT

The present study focuses on the biosorption of methyl violet (MV) from aqueous solution using an Algerian biomass, *Ammodaucus leucotrichus*. The biosorption of MV on *A. leucotrichus* was investigated as function of pH (3–10), stirring speed (100–400 rpm), biosorbent dosage (0.5–3 g L^{-1}), and initial MV concentrations (10–50 mg L^{-1}). All experiments were carried out in a batch reactor at room temperature. FTIR analysis of our biosorbent material showed the presence of main functional groups, amino, carboxyl, hydroxyl, and carbonyl groups, which are efficient biosorbents responsible for the removal of MV. The effects of biosorption were examined and the percentage of MV removal increased from ~68 to 93%. Pseudo-first-order, Elovich equation, and pseudo-second-order models were used to interpret and explain the experimental data. The sorption kinetics of MV onto *A. leucotrichus* biomass was explained by the pseudo-second-order kinetic equation. Freundlich, Langmuir, Dubinin–Radushkevich, and Temkin models were applied to describe the sorption isotherm. The obtained results indicated that the MV sorption follows the Freundlich models. Under the optimum conditions, the maximum biosorption capacity (q_{max}) was 500 mg g^{-1}.

Keywords: Ammodaucus leucotrichus; Biosorption; Methyl violet; Isotherm; Kinetic models

1. Introduction

One of the most hazardous substances discharged with wastewater are dyes, especially industrial dyes, which are used in many industrial sectors such as textile dyes, paper, leather, food, and the cosmetic industries [1–4]. In fact, synthetic dyes play a major part in our life as they are found in the various products ranging from clothes, leather accessories to furniture. Most of these dyes are toxic and dangerous for the environment, and their removal from wastewater is a major environmental challenge [5]. Many methods have been suggested to handle the dye removal from water; these include physicochemical, biological treatment, and advanced oxidation processes [6–10]. These processes may achieve positive results in the elimination of industrial effluents, but such methods are often very costly and not environmentally safe [11,12]. Using biosorption, as a technique, proved as the most acknowledged treatment method since it gives the best results and may be used to eliminate diverse range of dyes [13]. Biosorption is a physicochemical process based on a variety of mechanisms including absorption, adsorption, ion exchange, and precipitation. Biosorption processes are conventional biotreatment processes highly important

---

*Corresponding author.

for the protection of our environment. So, different kinds of biosorbents have been used to eliminate inorganic- and organic-polluting biomaterials such as activated carbon (coal) derived from biomass [14,15]. Recently, other adsorbents which can be used as effective materials for removing cationic dyes from water are magnetic Fe_3O_4@graphene and core/shell $Fe_3O_4/SiO_2/GO$ materials. These materials have attracted much attention due to their unique properties such as chemical stability, magnetic response, low cytotoxicity, and biocompatibility as well as good dispersion with uniform particle size [16,17].

Compared to classical adsorbents such as activated carbon, carbon nanotubes (CNTs) are known as the best efficient materials to eliminate inorganic or organic contaminants from wastewater; this is due to their physicochemical stability, high selectivity, and also their structural variety [18]. However, this adsorbent is expensive to produce and hard to regenerate at times. As a result, it is necessary to explore other efficient and cheaper biosorbents. Microbial, plant, and animal biomass with different forms have received attention from researchers. For this reason, *Ammodaucus leucotrichus* (*A. leucotrichus*) used as biosorbent received much interest due to its efficiency, affordable cost, and abundance. *A. leucotrichus* is found in parts of the Saharan desert belonging to North African nations, namely Algeria, Morocco, and Tunisia; their seeds are used in these countries as traditional herbal medicine for cold, fever, and digestive complaints particularly in children [19,20]. Others kind of naturally occurring biosorbents have been used to remove dyes from wastewater and also for the purification of aquatic medium, namely algae [21], agricultural wastes [22], and plant wastes [23]. The aim of this work is to study the biosorption of methyl violet (MV) in the presence of *A. leucotrichus* as biosorbent. MV is widely employed in the Algerian textile as cosmetics, plastics, photographic, and also paper industry. *A. leucotrichus* was collected from the region of south Algeria. This biosorbent with a particles size between 10 and 15 mm has been used after stream distillation. The work is carried out under various experimental conditions such as initial pH, biosorbent amount, contact time, agitation, and initial dye concentration. The biosorption kinetics and isotherms have been studied to validate experimental data.

2. Experimental section

2.1. Biosorbent preparation

Ammodaucus leucotrichus (*Apiaceae*) was collected from the municipality of El Menia, located 267 km southwest of Ghardaia city, Algeria. Seeds of the plant with particles size between 10 and 15 mm were washed several times with bi-distilled water and then dried over night at 60℃. Finally, the obtained biosorbent was stored in a desiccator until use.

2.2. Preparation of aqueous dye solutions

MV was purchased from Aldrich Chemical Co., (USA) with purity >99.1%, its chemical formula is $C_{23}H_{26}N^3 + Cl^-$ and molar mass is 407.979 g mol^{-1}. The biosorption experiments were carried out under ambient conditions. MV was used without further purification; the stock solution was prepared by dissolving a weighed amount of a dye in 1,000 mL of bi-distilled water to obtain a concentration of 1,000 mg L^{-1}. Samples with various concentrations ranging from 10 to 50 mg L^{-1} were prepared by diluting the stock solution. The pH of each solution was adjusted to a desired value with HCl or NaOH solutions (0.1 N).

2.3. Kinetic studies

The experiments were performed in a set of 100-mL beakers that contain a definite volume of fixed initial dye's concentrations. The beakers were kept at room temperature (RT) under air with agitation speed of 300 rpm. The residual concentration was determined by UV–visible spectrophotometer (Specord 210 plus, Analytik jena) in 1-cm matched quartz cells. The maximum absorption wavelength was 588 nm. The dye amount adsorbed at equilibrium, q_e (mg g^{-1}), was calculated using the following equations:

$$q_t = \frac{C_0 - C_t}{m} \times V \qquad (1)$$

$$q_e = \frac{C_0 - C_e}{m} \times V \qquad (2)$$

The biosorption yield (Y) can be calculated using the equation:

$$Y(\%) = \frac{C_0 - C_e}{C_0} \times 100 \qquad (3)$$

where C_0, C_e, C_t, V, and m represent the initial concentration (mg L^{-1}), the final concentration (mg L^{-1}), the biosorbate concentration (mg L^{-1}) at time t (min), the volume of the solution (L), and the mass of adsorbent (g), respectively.

2.4. Characterization techniques

Fourier transform infrared (FTIR) spectra were recorded with a Bruker Alpha-p spectrometer over the range of 4,000–400 cm^{-1}. The surface morphology of *A. leucotrichus* was investigated by scanning electron microscopy (SEM) using an environmental SEM-type Quanta TM 250.

3. Results and discussion

3.1. Characterization of A. leucotrichus

FTIR spectroscopy analysis is an important technique to obtain appreciated information about functional groups of biosorbents. The identification of chemical groups involved in the sorption of *A. leucotrichus* before and after reaction was regrouped in Fig. 1(a) and (b). The results of fresh *A. leucotrichus* showed the presence of amine, alcohols, carboxylic, and ketones function playing an important role in the biosorption process (Fig. 1). The weak bands located at around 1,660 and 1,380 cm^{-1}, corresponded to C=O and C–O stretching vibrations associated with carboxylic groups (–COOH), while a broad peak at 1,016 cm^{-1} is attributed to a C–OH stretching vibration. The results show similar spectra suggesting that the *A. leucotrichus* structure remained intact after reaction. The broadband at ~3,320 cm^{-1} represented –OH groups of physisorbed water. The peaks observed around 2,918–2,965 cm^{-1} were assigned to the aliphatic C–H group. Symmetric bending of CH3 was observed at 1,434–1,241 cm^{-1}. The peaks observed at 1,010 and 538 cm^{-1}, corresponded to C–O stretching vibrations

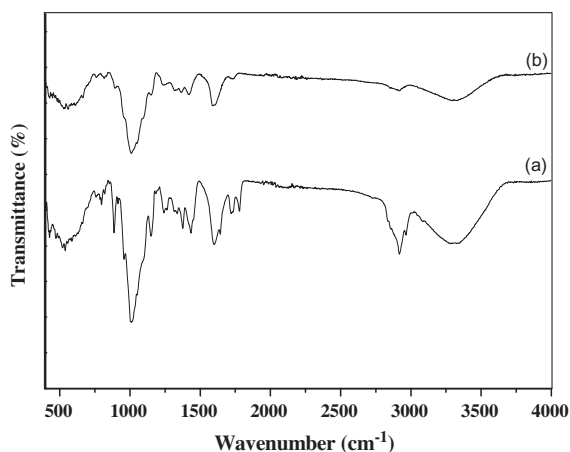of alcohol groups and –CN scissoring, respectively. The peaks around 1,600–1,770 cm^{-1} corresponds to the C=C stretch of aromatic cycle. Therefore, after *A. leucotrichus* biosorption, the bands between 1,605 and 1,007 cm^{-1} did not shift. The band intensity at 800, 889, 1,157, 1,232, 1,383, 1,438, 1,727, 1,781, and 2,968 cm^{-1} decreased, indicating the reaction between *A. leucotrichus* and MV functions such as hydroxyl, amine, CH2, C–H, and carboxylic groups.

The surface structure of the fresh biosorbent *A. leucotrichus* was analyzed by SEM (Fig. 2). SEM images clearly show that the *A. leucotrichus* surface exhibited different surface morphologies with a non-homogeneous distribution (Fig. 2(c) and (d)).

3.2. Effect of initial pH

The initial pH effect on the biosorption process was investigated in the pH range (3–10) (Fig. 3). As the pH value increased from 3 to 5, the removal efficiency also increased and reached a maximum value (83.5%). On the other hand, the efficiency decreased when the pH value passed from 5 to 10. This result indicated that the biosorption depending on pH may be explained by the point zero charge (pH$_{pzc}$). pH$_{pzc}$ plays an important role in explaining the biosorption mechanism [24]. In our case, the pH$_{pzc}$ (equal to 4.2) of *A. leucotrichus* biosorbent was measured using the solid addition method [25]. This result indicated that the treatment efficiency of MV in the presence of the biomass depend on the pH value and also on the charge distribution over the biomass surface [26–28]. The pH$_{pzc}$ indicated that the biosorbent surface is positively charged at pH less than 5, however, pH greater than 5 results in a negatively charged surface. Indeed, a high electrostatic attraction phenomenon existed between positively charged cationic dye and the negatively charged *A. leucotrichus* surface at pH 4.2 due to the ionization of functional *A. leucotrichus* groups. So, pH increased the number of negatively charged sites due to the presence of carbonate group [29].

3.3. Effect of stirring speed

In the biosorption process, agitation is an important parameter that can influence the pollutant distribution in the solution. To investigate this effect on MV biosorption, the experiments were performed under different stirring speed; 100, 200, 300, and 400 rpm at RT. As the stirring speed increased and reached a maximum at 300 rpm, the removal efficiency reached 83.5% and then decreased to 67.7% at
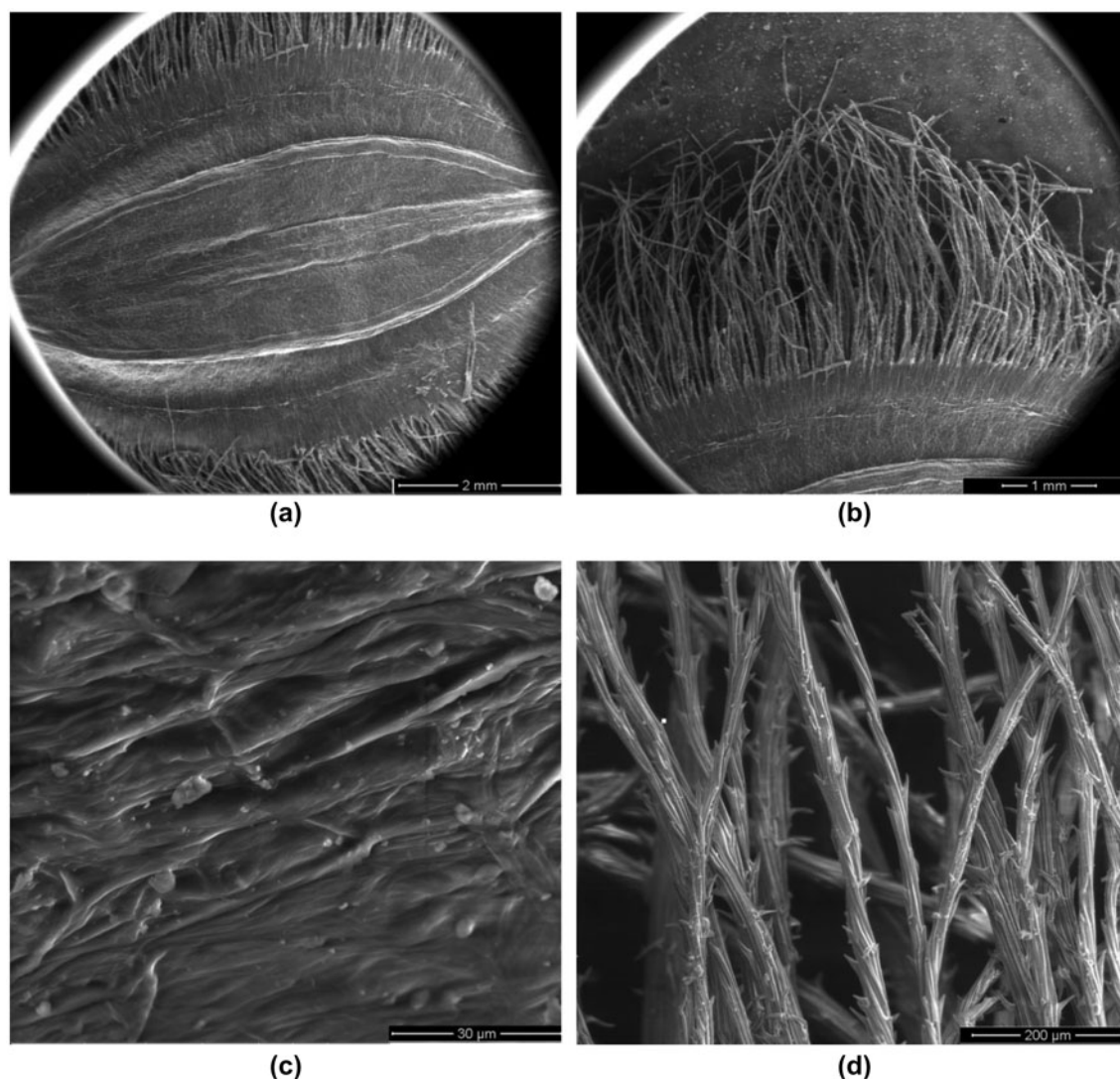

Fig. 1. FTIR spectra of *A. leucotrichus*, (a) before and (b) after biosorption.

Fig. 2. (a–d) Scanning electron microscopy (SEM) image of the biomass at differents region with various magnifications.

400 rpm (Fig. 4). This result may be due to the flow layer stability presented on *A. leucotrichus* surface. Also, the increase in the stirring rate reduced the liquid thickness.

3.4. Effect of MV concentration and the contact time on A. leucotrichus biosorption

In order to determine the relationship between MV concentration and *A. leucotrichus* biosorption efficiency, the initial MV concentration was varied from 10 to 50 mg L^{-1} at RT using 1 g L^{-1} of biosorbent. It was obvious that the amount of adsorbed material increased with the initial MV concentration where the adsorption capacity was dependent on the initial concentration. The sorption capacity at equilibrium, q_e, increased from 9.58 to 41.88 mg g^{-1}, while the initial concentration passed from 10 to 50 mg L^{-1} (Fig. 5). The optimum time was carried out at pH 5 with an initial MV concentration 50 mg L^{-1}, 1 g L^{-1} of biosorbent dosage and in the time range (5–180 min). As shown in Fig. 5, the biosorption was rapidly increased in the first 50 min involving physical adsorption at the biosorbent surface. After the initial step, the biosorption moderately increased due to the saturation of binding sites or a slow intracellular diffusion [30]. The equilibrium was attained near 180 min when maximum dye adsorption capacity reached 93.83%.
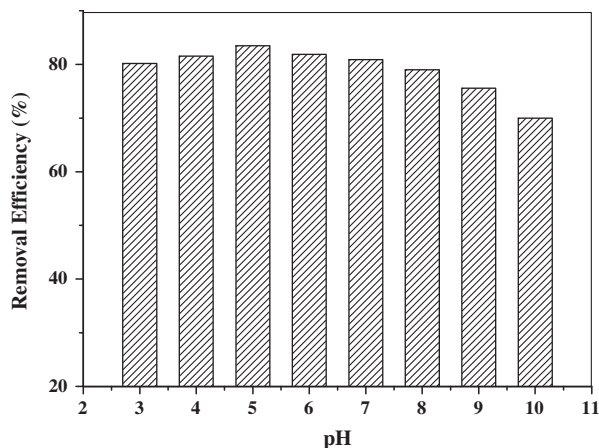
Fig. 3. Effect of pH value on the efficiency biosorption removal of MV after 180 min of reaction: $C_0 = 50$ mg L^{-1}, *A. leucotrichus* dose = 1 g L^{-1}, and stirring rate of 300 rpm.

Fig. 5. Effect of initial concentration of MV on the efficiency biosorption removal of MV vs. time: Stirring speed = 300 rpm, *A. leucotrichus* dose = 1 g L^{-1}, and pH 5: (□) 10, (○) 20, (△) 30, (▽) 40, and (◇) 50 mg L^{-1}. Inset: curves evolution in the time region (0–60) min.
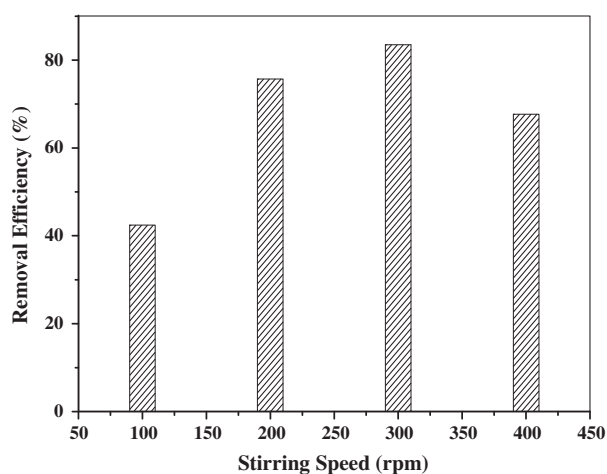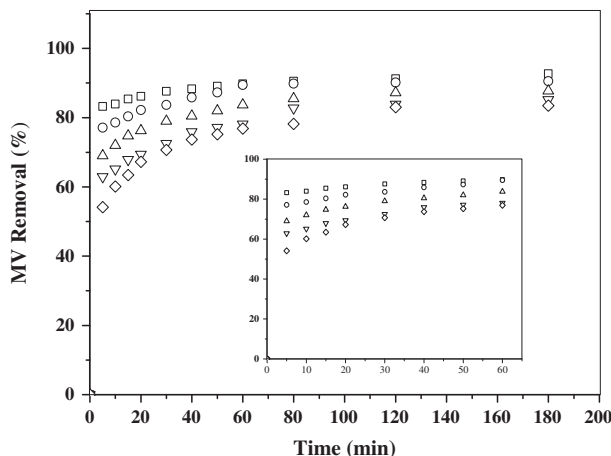

Fig. 4. Effect of stirring speed value on the efficiency biosorption removal of MV after 180 min of reaction under reaction conditions: $C_0 = 50$ mg L^{-1}, *A. leucotrichus* dose = 1 g L^{-1}, and pH 5.
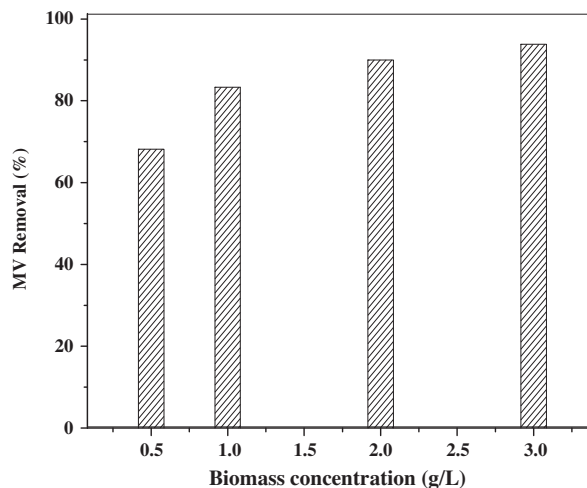

Fig. 6. Effect of bioadsorbent dose on the efficiency removal of MV after 180 min of reaction under reaction conditions: stirring speed = 300 rpm, $C_0 = 50$ mg L^{-1}, and pH 5.

3.5. Effect of A. leucotrichus dosage

The effect of *A. leucotrichus* dosage on the removal of MV from aqueous solutions was investigated with a dye concentration of 50 mg L^{-1}. The adsorbent dosage was varied from 0.5 to 3 g L^{-1}. The results shown in Fig. 6 illustrated that the removal efficiency increased by increasing the *A. leucotrichus* dose. After 180 min of reaction, the efficient dye removal was varied from 68.20% for 0.5 g L^{-1} to 93.83% for 3 g L^{-1} due to the increase in the site number available for dye biosorption. As mentioned in Fig. 6, the elimination was not significant when *A. leucotrichus* dose was higher than 2 g L^{-1}.

3.6. Biosorption kinetics

Three kinetic models were applied to adsorption kinetic data in order to investigate the behavior of adsorption process of MV dye onto *A. leucotrichus*. These models are the pseudo-first-order, Elovich equation, and pseudo-second-order. These models were most commonly used to describe the kinetic models for the dyes sorption [31–33].

3.6.1. Pseudo-first-order model

The pseudo-first-order kinetic model is generally more suitable when the solute concentration is low. The kinetic model of the pseudo-first-order is given as [34]:

$$\frac{dq_t}{dt} = k_1 (q_e - q_t) \tag{4}$$

where q_t, q_e, and k_1 are the amount of biosorbate sorbed at time t (mg g^{-1}), the biosorption capacity in equilibrium (mg g^{-1}), and the rate constant of pseudo-first-order model (min^{-1}), respectively.

The integrated form of the model for the boundary conditions ($q_t = 0$ at $t = 0$ and $q = q_t$ at $t = t$) has the following form [35]:

$$\ln (q_e - q_t) = \ln q_e - \frac{K_1}{2.0303} \times t \tag{5}$$

The straight line plots of $\ln (q_e - q_t)$ vs. time have been used to obtain the rate parameters. The values of k_1 and correlation coefficient (R^2) of the dye solutions at different concentrations were calculated from these plots (Table 1). From these results, it was clear that the equilibrium capacity q_e increased with increasing initial dye concentration. R^2 values were augmented from 0.631 to 0.919, while the concentration increased from 10 to 50, respectively. So, these results indicated that the biosorption did not follow the first-order kinetic.

3.6.2. Elovich equation

The Elovich equation is given as follows [35]:

$$\frac{dq_t}{dt} = \alpha \exp (-\beta q_t) \tag{6}$$

where α, β are the initial sorption rate (mg g^{-1} min^{-1}) and the desorption constant (g mg^{-1}), respectively. To

simplify the Elovich equation, it is assumed that $(\alpha \beta t) >> 1$, thus, the equation becomes as the follow:

$$q_t = \frac{1}{\beta} \ln (\alpha \beta) + \frac{1}{\beta} \ln t \tag{7}$$

The constant can be obtained from the slope and intercept of the straight line plot of q_t vs. $\ln (t)$. From Elovich equation, R^2 have changed within range (0.9512–0.9894) (Table 1). Therefore, the experimental data did not fit with the Elovich equation.

3.6.3. Pseudo-second-order model

The biosorption can also be described by pseudo-second-order kinetic model. The pseudo-second-order model can be evaluated from the following equation [36]:

$$\frac{dq_t}{dt} = k_2 (q_e - q_t)^2 \tag{8}$$

where k_2 is the pseudo-second-order rate constant (g mg^{-1} min^{-1}).

After integrating Eq. (8) using the boundary conditions, the following formula is obtained:

$$\frac{t}{q_t} = \frac{1}{k_2 q_e^2} + \frac{t}{q_e} \tag{9}$$

A plot of t/q_t vs. time should give a linear relationship if the biosorption follows pseudo-second-order model. k_2 and q_e can be calculated from the slope and intercept of the plots t/q_t vs. time, respectively (Fig. 7). The results of pseudo-second-order plot at various initial dye concentrations are regrouped in Table 1. R^2 values were close to one compared to the pseudo-first-order kinetic model and the Elovich equation. Good correlation coefficients were obtained by

Table 1
Constant of kinetic models

| Con. mg L^{-1}	$q_{e,exp}$ mg g^{-1}	Pseudo-first-order model			Elovich equation			Pseudo-second-order model		
		$k_1 \times 10^2$ min^{-1}	$q_{e,mod}$ mg g^{-1}	R^2	α mg g^{-1} min^{-1}	β g mg^{-1}	R^2	$k_2 \times 10^2$ g mg^{-1} min^{-1}	$q_{e,mod}$ mg g^{-1}	R^2
10	9.58	2.291	1.201	0.631	4.340×10^{11}	3.454	0.9886	6.386	9.60	0.9999
20	18.78	3.492	1.975	0.873	5.659×10^6	1.088	0.9512	2.655	19.01	0.9999
30	26.47	3.025	2.589	0.908	5.660×10^4	0.579	0.9882	1.172	26.88	0.9997
40	34.63	2.558	3.106	0.898	5.528×10^3	0.351	0.9755	0.605	35.33	0.9993
50	41.87	3.045	3.778	0.919	4.928×10^2	0.231	0.9894	0.423	42.92	0.9992
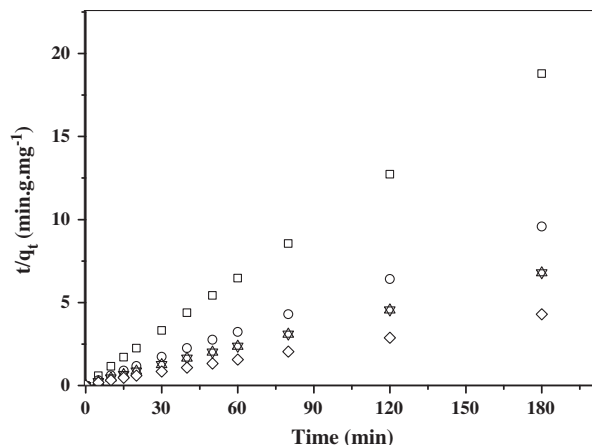
Fig. 7. Evolution of t/q_t vs. time at different dye concentrations: (□) 10, (○) 20, (△) 30, (▽) 40, and 50 (◇).

fitting the experimental data, indicating that the adsorption process for MV was the pseudo-second-order. Similar phenomena have been observed in the biosorption of different kinds of dye [35–41]. MV biosorption on *A. leucotrichus* is therefore described by pseudo-second-order model kinetic with very high correlation coefficient.

3.7. Adsorption equilibrium study

Equilibrium isotherm equations are used to describe the experimental biosorption data and the parameters obtained from the different models. The isotherm equations used to describe the equilibrium nature of MV biosorption on *A. leucotrichus* biosorption are Freundlich, Langmuir, Dubinin–Radushkevich, and Temkin equations.

3.7.1. Freundlich and Langmuir isotherms

The Freundlich isotherm is based on a heterogeneous adsorption surface with different adsorption energy sites, whereas the Langmuir isotherm is based on the hypothesis that the adsorption energy is constant and independent of surface coverage. The Freundlich isotherm is derived by assuming a heterogeneous Langmuir [42]. The linearized form of Freundlich and Langmuir isotherms can be represented by the Eqs. (10) and (11):

$$\ln q_e = \ln K_F + \frac{1}{n} \ln C_e \quad (10)$$

$$\frac{1}{q_e} = \frac{1}{q_m} + \frac{1}{K_L q_m} \frac{1}{C_e} \quad (11)$$

where K_F, n, K_L, and q_m are the Freundlich constant (L mg^{-1}), biosorption intensity, the Langmuir adsorption constant (L mg^{-1}) related to energy of adsorption and signifies adsorption capacity (mg g^{-1}), respectively.

Fig. 8 regrouped Freundlich (ln (q_e) vs. ln (C_e)) and Langmuir (1/q_e vs. 1/C_e) plots. The parameter values are regrouped in Table 2. In all cases, the Freundlich equation represented a better fit of experimental data compared to the Langmuir equation. Biosorption intensity n ~ 1 illustrated that the biosorbate was favorably biosorbed on the *A. leucotrichus* [43].

3.7.2. Dubinin–Radushkevich isotherm

Another equation was used in the analysis of isotherms proposed by Dubinin–Radushkevich (D–R) [44]:

$$q_e = q_m \exp\left(-k_{D-R}\, \varepsilon^2\right) \quad (12)$$

where k_{D-R} is a constant and ε can be correlated:

$$\varepsilon = RT \ln\left(1 + \frac{1}{C_e}\right) \quad (13)$$

The linearized Dubinin–Radushkevich (D–R) isotherm is represented by the following equation:

$$\ln q_e = \ln q_m - k_{D-R}\, \varepsilon^2 \quad (14)$$

The constant k_{D-R} gives the mean free energy E of sorption per molecule of sorbate when it is transferred to the material surface from infinity in the solution [45]:

$$E = \frac{1}{\sqrt{2k_{D-R}}} \quad (15)$$

Dubinin–Radushkevich constants were shown in Table 2. The D–R isotherms were plotted against the experimental data points (Fig. 8). It was clear that the sorption energy value was lower than the sorption capacity of MV. R^2 value was much lower compared to other isotherms values.

3.7.3. Temkin isotherm

Temkin isotherm contains a factor that explicitly takes into account sorbing species and sorbate interactions. This isotherm assumes that the biosorption heat

of all molecules in the layer decreases linearly due to adsorbate/adsorbate interactions, Temkin isotherm equation is:

$$q_e = \frac{RT}{b} \ln (K_T C_e) \tag{16}$$

This equation can be expressed in its linear form as:

$$q_e = B_1 \ln K_T + B_1 \ln C_e \tag{17}$$

where

$$B_1 = \frac{RT}{b} \tag{18}$$

The sorption data can be analyzed according to Eq. (17). A plot of q_e vs. ln (C_e) enables the determination of isotherm constants, K_T and B_1, from the slope and intercept of the plot, respectively. K_T is the equilibrium-binding constant corresponding to the maximum binding energy (L g^{-1}) and constant B_1 is related to the heat of biosorption (J mg^{-1}) (Table 2). So, the comparison between different isotherm models shown that, the most satisfactory prediction of MV biosorption onto *A. leucotrichus* was provided by the Langmuir model with a highest correlation coefficient ($R^2 > 0.999$), while the lowest one was D–R equation. Indeed, the constants and correlation coefficients R^2 values obtained from the four models applied for biosorption of MV on *A. leucotrichus* (Table 2) shown that Langmuir and Freundlich models gave the
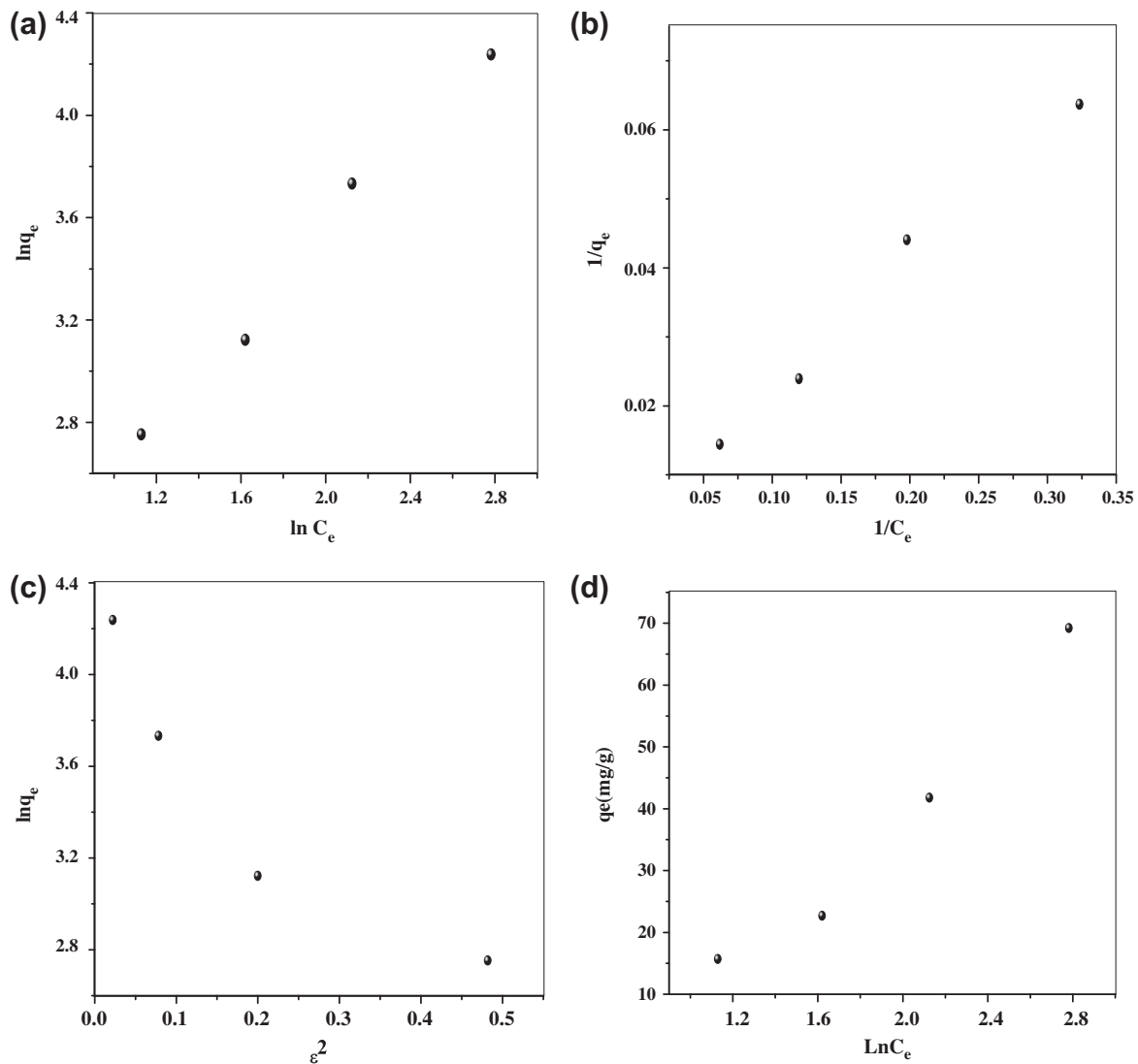

Fig. 8. Evolution of (A) ln q_e vs. ln C_e, (B) $1/q_e$ vs. $1/C_e$, (C) ln q_e vs. ε^2, and (D) q_e vs. ln C_e.

Table 2
Constants of Freundlich, Langmuir, Dubinin–Radushkevich, and Temkin isotherms models

Isotherms Models	Models constants	Value
Langmuir	q_m (mg g^{-1})	500
	K_L (L mg^{-1})	0.0104
	R^2	0.989
	R_L	0.657
Freundlich	K_F (L mg^{-1})	5.430
	R^2	0.9913
	N	1.082
Dubinin–Radushkevich	q_m (mg g^{-1})	1.395
	K_{D-R} (mol k^{-1} J^{-1})^2	2.947
	R^2	0.845
	E (kJ mol^{-1})	0.412
Temkin	B_1 (J mol^{-1})	33.28
	B	74.5
	R^2	0.965
	K_t (L g^{-1})	9.38

highest R^2 compared to the D–R and Temkin model. The maximum value of sorption capacity (q_m) 500 mg g^{-1} was obtained for Langmuir model.

3.8. Comparison with other sorbents

A comparison of the sorption capacity q_m (mg g^{-1}) of a few adsorbents available in literature for removal of MV from aqueous solutions was regrouped in Table 3. It was clear that A. leucotrichus biosorbent used in the present work had a relatively high sorption capacity compared to other sorbents. So, A. leucotrichus is a suitable biomass for the removal of MV from aqueous solutions with q_m = 500 mg g^{-1}.

Table 3
Comparison of maximum adsorption capacities of A. leucotrichus with other adsorbents for MV in aqueous solutions

Adsorbents	q_m (mg g)	Refs.
Activated carbon	500	[46]
N-benzyltriazole derivatized dextran	95.24	[47]
Sunflower seed hulls	92.59	[48]
Halloysite nanotubes	105.26	[49]
Puerh tea powder	277.78	[50]
Halloysite nanotube-Fe$_3$O$_4$	90.09	[51]
Ammodaucus leucotrichus	500	Present study

4. Conclusion

The present work was designed to investigate the biosorption behavior of MV onto the A. leucotrichus. The maximum biosorption capacity was 93.83% at optimum operating conditions. FTIR indicated that the amino, carboxyl, hydroxyl, and carbonyl groups on the surface of the biomass are responsible for biosorption of MV. Based on these results, A. leucotrichus biomass can be used as an efficient low-cost biosorbent for the removal of MV dye from wastewater. The pseudo-second-order kinetic equation could best describe the biosorbent kinetics, and Freundlich isotherm model best fit onto the experimental data with a maximum biosorption capacity q_{max} = 500 mg g^{-1}.

References

[1] H. Zollinger, Synthesis, properties of organic dyes and pigments, in: Color Chemistry, VCH Publishers, New York, NY, 1987, pp. 92–102.

[2] P.A. Carneiro, R.F.P. Nogueira, M.V.B. Zanoni, Homogeneous photodegradation of C.I. Reactive Blue 4 using a photo-Fenton process under artificial and solar irradiation, Dyes Pigm. 74 (2007) 127–132

[3] H. Ben Mansour, D. Corroler, D. Barillier, K. Ghedira, L. Chekir, R. Mosrati, Evaluation of genotoxicity and pro-oxidant effect of the azo dyes: Acids yellow 17, violet 7 and orange 52, and of their degradation products by Pseudomonas putida mt-2, Food Chem. Toxicol. 45 (2007) 1670–2677.

[4] K.T. Chung, C.E. Cerniglia, Mutagenicity of azo dyes: Structure-activity relationships, Mutat. Res. Rev. Genet. Toxicol. 277 (1992) 201–220.

[5] S.R. Rodríguez Couto, Dye removal by immobilised fungi, Biotechnol. Adv. 27 (2009) 227–235.

[6] A. Szygu1a, E. Guibal, M.A. Palacin, M. Ruiz, A.M. Sastre, Removal of an anionic dye (Acid Blue 92) by coagulation–flocculation using chitosan, J. Environ. Manage. 90 (2009) 2979–2986.

[7] M. El Haddad, R. Mamouni, N. Saffaj, S. Lazar, Removal of a cationic dye—Basic Red 12—From aqueous solutions by adsorption onto animal bone meal, J. Assoc. Arab. Univ. Basic. Appl. Sci. 12 (2012) 48–54.

[8] M. Karatas, Y.A. Argun, M.E. Argun, Decolorization of antraquinonic dye, Reactive Blue 114 from synthetic wastewater by Fenton process: Kinetics and thermodynamics, J. Ind. Eng. Chem. 18 (2012) 1058–1062.

[9] E. Alventosa-deLara, S. Barredo-Damas, M.I. Alcaina-Miranda, M.I. Iborra-Clar, Ultrafiltration technology with a ceramic membrane for reactive dye removal: Optimization of membrane performance, J. Hazard. Mater. 209–210 (2012) 492–500.

[10] G. Sudarjanto, B.K. Lehmann, J. Keller Optimization of integrated chemical-biological degradation of a reactive azo dye using response surface methodology, J. Hazard. Mater. B 138 (2006) 160–168.

[11] P. Nigam, I.P. Banat, D. Singh, R. Marchant, Microbial process for the decolorization of textile effluent containing azo, diazo and reactive dyes, Process Biochem. 31 (1996) 435–442.

[12] M.A. Rauf, I.A. Shehadi, W.W. Hassan, Studies on the removal of Neutral Red on sand from aqueous solution and its kinetic behavior, Dyes Pigm. 75 (2007) 723–726.

[13] Z.M. Magriotis, S.S. Vieira, A.A. Saczk, N.A.V. Santos, N.R. Stradiotto, Removal of dyes by lignocellulose adsorbents originating from biodiesel production, J. Environ. Chem. Eng. 2 (2014) 2199–2210.

[14] G.M. Gadd, Biosorption: Critical review of scientific rationale, environmental importance and significance for pollution treatment, J. Chem. Technol. Biotechnol. 84 (2009) 13–28.

[15] R. Dhankhar, A. Hooda, Fungal biosorption—An alternative to meet the challenges of heavy metal pollution in aqueous solutions, Environ. Technol. 32 (2011) 467–491.

[16] Y.Y.S. Miao, S. Yu, L.P. Ma, H. Sun, S. Wang, Fabrication of Fe_3O_4/SiO_2 core/shell nanoparticles attached to graphene oxide and its use as an adsorbent, J. Colloid Interface Sci. 379 (2012) 20–26.

[17] Y. Yao, S. Miao, S. Liu, L.P. Ma, H. Sun, S. Wang, Synthesis, characterization, and adsorption properties of magnetic Fe_3O_4@graphene nanocomposite, Chem. Eng. J. 184 (2012) 326–332.

[18] Y. Yao, H. Bing, X. Feifei, C. Xiaofeng, Equilibrium and kinetic studies of methyl orange adsorption on multiwalled carbon nanotubes, Chem. Eng. J. 170 (2011) 82–89.

[19] B. Muckensturm, F. Diyani, D. Nouën, S. Fkih-Tetouani, J.P. Reduron, Ammolactone, a guaianolide from a medicinal plant, *Ammodaucus leucotrichus*, Phytochemistry 44 (1997) 907–910.

[20] I.A. El-Haci, C. Bekhechi, F. Atik-Bekkara, W. Mazari, M. Gherib, A. Bighelli, J. Casanova, F. Tomi, Antimicrobial activity of *Ammodaucus leucotrichus* fruit oil from Algerian Sahara, Nat. Prod. Commun. 9 (2014) 711–712.

[21] Z. Bekçi, Y. Seki, L. Cavas, Removal of malachite green by using an invasive marine alga *Caulerpa racemosa* var. *cylindracea*, J. Hazard. Mater. 161 (2009) 1454–1460.

[22] Z. Aksu, I.A. Isoglu, Use of agricultural waste sugar beet pulp for the removal of Gemazol turquoise blue-G reactive dye from aqueous solution, J. Hazard. Mater. 137 (2006) 418–430.

[23] C.H. Weng, Y.T. Lin, T.W. Tzeng, Removal of methylene blue from aqueous solution by adsorption onto pineapple leaf powder, J. Hazard. Mater. 170 (2009) 417–424.

[24] M. El Haddad, A. Regti, R. Slimani, S. Lazar, Assessment of the biosorption kinetic and thermodynamic for the removal of safranin dye from aqueous solutions using calcined mussel shells, J. Ind. Eng. Chem. 20 (2014) 717–724.

[25] I.D. Mall, V.C. Srivastava, G.V.A. Kumar, I.M. Mishra, Characterization and utilization of mesoporous fertilizer plant waste carbon for adsorptive removal of dyes from aqueous solution, Colloiods Surf., A Physicochem. Eng. Aspects 278 (2006) 175–187.

[26] M. Alkan, Ö. Demirbaş, M. Doğan, Electrokinetic properties of sepiolite suspensions in different electrolyte media, J. Colloid Interface Sci. 281 (2005) 240–248.

[27] M. Doğan, Y. Özdemir, M. Alkan, Adsorption kinetics and mechanism of cationic ethyl violet and methylene blue dyes onto sepiolite, Dyes Pigm. 75 (2007) 701–713.

[28] S. Arellano-Cárdenas, S. López-Cortez, M. Cornejo-Mazón, J. Carlos Mares-Gutiérrez, Study of malachite green adsorption by organically modified clay using a batch method, Appl. Surf. Sci. 280 (2013) 74–148.

[29] M. Ghaedi, S. Hajati, B. Barazesh, F. Karimi, G. Ghezelbash, Equilibrium, kinetic and isotherm of some metal ion biosorption, J. Ind. Eng. Chem. 19 (2013) 227–233.

[30] B.H. Hameed, Equilibrium and kinetic studies of methyl violet sorption by agricultural waste, J. Hazard. Mater. 154 (2008) 204–212.

[31] Y.S. Ho, G. McKay, Pseudo-second order model for sorption processes, Process Biochem. 34 (1999) 451–465.

[32] N. Kannan, M. Sundaram, Kinetics and mechanism of removal of methylene blue by adsorption on various carbons a comparative study, Dyes Pigm. 51 (2001) 25–40.

[33] Q. Sun, L. Yang, The adsorption of basic dyes from aqueous solution on modified peat–resin particle, Water Res. 37 (2003) 1535–1544.

[34] S. Lagergren, About the theory of so-called adsorption of soluble substances, K Svenska Vetenskapsakademiens, Handlingar 24 (1898) 1–39.

[35] E. Augustine Ofomaja, Kinetic study and sorption mechanism of methylene blue and methyl violet onto mansonia (*Mansonia altissima*) wood sawdust, Chem. Eng. J. 143 (2008) 85–95.

[36] Y.S. Ho, G. McKay, Pseudo-second order model for sorption processes, Process Biochem. 34 (1999) 451–465.

[37] Z. Aksu, S. Tezer, Equilibrium and kinetic modelling of biosorption of Remazol Black B by *Rhizopus arrhizus* in a batch system: Effect of temperature, Process Biochem. 36 (2000) 431–439.

[38] C. Namasivayam, D. Kavitha, Removal of Congo Red from water by adsorption onto activated carbon prepared from coir pith, an agricultural solid waste, Dyes Pigm. 54 (2002) 47–58.

[39] M. Alkan, M. Doğan, Adsorption kinetics of victoria blue onto perlite, Fresenius Environ. Bull. 12(5) (2003) 418–425.

[40] M. Doğan, M. Alkan, Adsorption kinetics of methyl violet onto perlite, Chemosphere 50 (2003) 517–528.

[41] M. Doğan, M. Alkan, A. Turkyilmaz, Y. Özdemir, Kinetics and mechanism of removal of methylene blue by adsorption onto perlite, J. Hazard. Mater. B 109 (2004) 141–148.

[42] I. Langmuir, The adsorption of gases on plane surfaces of glass, mica and platinum, J. Am. Chem. Soc. 40 (1918) 1361–1403.

[43] V.K. Gupta, I. Ali, Utilisation of bagasse fly ash (a sugar industry waste) for the removal of copper and zinc from wastewater, Sep. Purif. Technol. 18 (2000) 131–140.

[44] S.D. Faust, O.M. Aly, Adsorption Processes for Water Treatment, Butterworth Scientific Ltd, Guidford, 1987, pp. 509.

[45] S.M. Hasany, M.H. Chaudhary, Sorption potential of Haro river sand for the removal of antimony from acidic aqueous solution, Appl. Radiat. Isot. 47 (1996) 467–471.

[46] S. Chen, J. Zhang, C. Zhang, Q. Yue, Y. Li, C. Li, Equilibrium and kinetic studies of methyl orange and methyl violet adsorption on activated carbon derived from *Phragmites australis*, Desalination 252 (2010) 149–156.

[47] E. Cho, M.N. Tahir, H. Kim, J.H. Yu, S. Jung, Removal of methyl violet dye by adsorption onto N-benzyltriazole derivatized dextran, RSC Adv. 43 (2015) 327–334.

[48] B.H. Hameed, Equilibrium and kinetic studies of methyl violet sorption by agricultural waste, J. Hazard. Mater. 154 (2008) 204–212.

[49] R. Liu, B. Zhang, D. Mei, H. Zhang, J. Liu, Adsorption of methyl violet from aqueous solution by halloysite nanotubes, Desalination 268 (2011) 111–116.

[50] P. Li, Y.J. Su, Y. Wang, B. Liu, L.M. Sun, Bioadsorption of methyl violet from aqueous solution onto Pu-erh tea powder, J. Hazard. Mater. 179 (2010) 43–48.

[51] J. Duan, R. Liu, T. Chen, B. Zhang, J. Liu, Halloysite nanotube-Fe_3O_4 composite for removal of methyl violet from aqueous solutions, Desalination 293 (2012) 46–52.